Impurity Penetration and Contamination in Tore Supra Ergodic Divertor Experiments

R. Guirlet, J. Hogan[1], P. Monier-Garbet, Y. Corre, C. De Michelis, P. Ghendrih, R. Giannella, C. Grisolia, A. Grosman, J. Gunn, B. Schunke and Tore Supra Team

Association Euratom-CEA sur la Fusion, C.E. Cadarache, 13108 St-Paul-lès-Durance, France
[1]Oak Ridge National Laboratory, Fusion Energy Division, PO Box 2009, Oak Ridge, TN37831-8072, USA

e-mail contact: guirlet@drfc.cad.cea.fr

Abstract. The screening effect of Ne and C in ergodic divertor plasmas is studied. Spectroscopic measurements show that the screening mechanism is not the same for the two impurities. A 2D model explains this difference by the longer penetration length of neutral Ne. 3D modelling of the plasma edge with the BBQ code confirms the brightness profile shape dependence on the edge T_e. The 1D impurity transport code MIST coupled to BBQ interprets the screening effect as posssibly due to strong impurity outfluxes coming out of the ergodic region.

1. Introduction

The ergodic divertor (ED) of Tore Supra (TS) has been proven to be an efficient tool to screen the confined plasma from intrinsic and injected impurities [1]. It creates a weak confinement region at the plasma edge by opening the field lines over the last centimetres of the plasma. In the outer part of this region, transport is laminar, and flux tubes with short and long connection lengths to the wall are intricate. In the inner part, transport and connection lengths are still random although longer. The particle behaviour is thus complex and an exact description is very difficult. In order to explain the role of the weak confinement region on impurity penetration and contamination, we first present a heuristic model showing the role of the weak confinement region width compared to the particle penetration depth. We then discuss the measurements and interpret them by modelling (2D and 3D) the penetration dependence on the plasma edge parameters. Finally 3D modelling of the sources coupled to a 1D impurity transport code is used to interpret the preceding results in terms of transport.

2. Model of the ergodic divertor plasma

A heuristic model [2] can be used to characterise the effective width of the weak confinement region. In this model, two zones describe entirely the plasma: the first one (width Δ_{eff}) corresponds to the plasma edge, interacting with the limiting components (in the present case, the ED neutraliser plates (NP), surface $S_{NP} \approx 0.65$ m^2, which take 30% of the heat flux [3]). The screening process is assumed to take place in this zone, and it is described by the exponential decay of the particle flux in the radial direction, with an e-folding length d_p: $\Phi_{in}(x) = \Phi_0 \cdot \exp(-x/d_p)$, where $\Phi_0 = n_Z^0 \cdot v_Z^0$ is the neutral flux emitted from the NP. The second zone represents the core plasma, where the number of particles coming out of the confined plasma is given by $(dN_Z/dt)_{out} = \langle n_Z^{core} \rangle \cdot V/\tau_Z$, where $\langle n_Z^{core} \rangle$ is the volume average core particle density, V the plasma volume and τ_Z the particle lifetime. At equilibrium we have $\Phi_{in}(x=\Delta_{eff}) \cdot S_{NP} = (dN_Z/dt)_{out}$, from which we obtain: $\Delta_{eff} = d_p \cdot \ln(n_Z^0 \cdot v_Z^0 / \langle n_Z^{core} \rangle \cdot \tau_Z \cdot S_{NP}/V)$. In the following we shall determine each of the parameters needed to calculate Δ_{eff}, either from measurements or from modelling.

3. Spectroscopic observation of neutral penetration

The experiments analysed for this purpose were performed with Deuterium plasmas in ED configuration. The electron density was ramped up by means of D_2 gas injection. Carbon and Neon have been studied separately in two different series of pulses. In the Neon series, 100 ms Neon puffs were injected at the beginning of the density ramp-up. All Neon densities quoted here are normalised to the amount of injected Neon (in Pa.l). One of the NPs is observed with a set of 4 optical fibres providing the radial brightness profiles of chosen spectral lines, such as C I (9080 Å multiplet) and Ne I (5852 Å), as shown on Fig. 1. Both impurities show the same type of spatial decay length, despite the difference in their ionisation potentials (C: 11.3 eV, Ne: 21.6 eV), a hint to the role of the particle emission velocity in the penetration process. It can also be seen that, when the edge temperature (T_e^{edge}, measured by a Langmuir probe on the NP) is decreased, the C I brightness profile becomes more peaked towards the plate, while the Ne I brightness maximum moves away from the NP. For Carbon, this can be explained by the fact that decreasing T_e^{edge} will decrease v_C^0 and increase n_e^{edge}, both resulting in a decreased neutral penetration, while the ionisation rate decreases only moderately in this temperature range (factor of 3). For Neon, this qualitative discussion is not sufficient because the v_{Ne}^0 (deduced from the Ne I line Doppler shift) exhibits a non-monotonic dependence on T_e^{edge} (not predicted by the TRIM code [4]) and the ionisation rate coefficient varies by a factor larger than 10.

4. Impurity penetration modelling

The brightness profiles give only a qualitative idea about the impurity penetration depth. To estimate this depth and compare it to the laminar layer width, a model of the plasma in the NP vicinity is necessary. In the 2D model used here, a realistic T_e distribution is deduced from the magnetic configuration computation performed by the MASTOC code [5], and an exponential radial profile of n_e with $\lambda_n = 3$ cm is deduced from Langmuir probe measurements [6]. On Fig. 2, the obtained penetration depth, d_p, is shown for neutral C and Ne atoms generated by the most energetic processes (physical sputtering for C, fast reflected for Ne: from 5 eV to 20 eV approximately), as a function of T_e^{edge}. In every case, despite the wide range of density and temperature values, d_p is seen to vary by less than a factor of 2. The trend for C as a function of T_e^{edge} is in agreement with the brightness profiles of Fig. 1. For Ne, d_p is generally larger than the estimated width of the outermost laminar region (approximately 4 cm), whereas for C, it is lower. This can explain the different behaviour of the species with respect to screening.

To model the impurity penetration depth, the 3D Monte-Carlo code BBQ [7] has also been used to take into account the complex 3D geometry of the NP and of the nearby plasma, as well as a realistic velocity distribution determined in part from TRIM reflection coefficients. BBQ starts from a flux of impurity neutrals determined from the measured incident particle flux onto the NP, taking into account the various neutral emission mechanisms (physical and chemical sputtering for Carbon, thermal and fast neutrals for Neon). Then BBQ follows the impurities as they enter the plasma and undergo transport and ionization to higher charge states in the plasma edge. The particle tracking is stopped when they have penetrated several centimetres into the ergodic zone. In agreement with the 2D model, the otained Carbon penetration depth decreases monotonically when the edge density is increased. For Neon, BBQ shows that the penetration probability from the emission location towards the ergodic zone increases slightly when T_e^{edge} is decreased, thus explaining the trend observed on the brightness profile.

5. Impurity densities and effective screening width

The different behaviour of Ne and C is illustrated by the comparison between the densities on the NP, deduced from the spectroscopic measurements, and the central densities (Fig. 3), deduced from the Lyα line of the corresponding Hydrogen-like ions observed along a plasma diameter. Note that the neutral Carbon density dependence on T_e^{edge}, as well as its absolute value, is matched by BBQ only if one assumes that Carbon self-sputtering is responsible for half the neutral Carbon density in the high T_e^{edge} range, i.e. when the Carbon flux onto the NP is a significant fraction of the Deuterium flux. The neutral Carbon density, together with the assumed dependence of the emission velocity on T_e^{edge}, indicates that the neutral Carbon flux decreases with T_e^{edge}, more or less at the same rate as the core Carbon density. Consequently, the screening effect in the case of Carbon seems to be related to the neutral generation process, and localised near the NP. The neutral Neon density is seen to be much more sensitive than Carbon to the edge parameters (variation by a factor of 10), with an opposite trend. It should be noticed that the large density increase concerns only a small part of the plasma ($<10^{-4}$ times total plasma volume). Therefore, it has not necessarily a large effect on the total Neon content. Neutral Ne velocity measurements (and TRIM reflection coefficients) show that the neutral Neon flux increases faster than the neutral density when T_e^{edge} is decreased. On the contrary, the core Neon density seems to be completely independent from the edge conditions, for a given Neon injection, indicating a screening intensity increasing with the edge density. The screening effect is thus effective but localised further inside the plasma.

The results obtained in the previous paragraphs are used to calculate the effective width of the perturbed layer Δ_{eff} introduced in the first part of this work. For both Carbon and Neon, d_p is taken from the 2D model, n_Z^0 and $<n_Z^{core}>$ from measurements, v_Z^0 from TRIM results. The particle lifetime τ_Z in the confined plasma is assumed to be 0.2 s, identical for both species and independent of the plasma conditions. The resulting Δ_{eff} is about 18 cm for Ne and less than 2 cm for C. For Neon, the useful region thus extends significantly further inside the plasma, suggesting that not only the laminar region but also the ergodic layer play a role in Ne screening. For Carbon, it confirms that the screening process takes place in a narrow region close to the NP, entirely contained in the laminar region. At 15 eV, when the neutral Carbon density starts increasing rapidly as the plasma approaches detachment, Δ_{eff} for C becomes larger than 2 cm. This suggests that Carbon screening is degraded close to detachment.

6. Impurity transport modelling

In order to interpret the preceding results in terms of transport, the BBQ results concerning the radial and poloidal distribution of ion charge states entering the core plasma and the corresponding fluxes are used as input to the 1D impurity transport code MIST [8] (Fig. 4). The measured T_e and n_e radial and time-dependent profiles from Thomson scattering are used, and edge profiles in the region $r/a > 0.86$ (where Thomson measurements are not available) are estimated from ECE measurements [9]. For Neon injection experiments, the MIST transport model is validated by a comparison with relative C and Ne CXRS brightness profiles [10] and with the absolute brightnesses of the Ne X, O VIII, C VI Lyα, C V R and I lines measured along a plasma diameter. The Carbon and Oxygen contributions to the total radiation are matched before Neon injection, and the incremental radiation due to Neon injection is matched using radiation rates from the ADAS database [11]. This allows the determination of the anomalous diffusivity and pinch velocity. To match the measurements, it is necessary to use a larger diffusion coefficient (by approximately a factor of 3) in the ergodic region. The result of the simulations (Fig. 5) is a core/SOL transport model in which

Neon penetrating from the SOL enters a region ($r/a_{Lim} > 0.75$) of enhanced outward diffusivity, leading to increased expulsion back to the SOL. The outward fluxes from the ergodic region have been checked to vary with the edge conditions in such a way that the Neon influx towards the core plasma remains rouhgly unchanged in all conditions. This is, thus, a plausible model to explain the observed decoupling between increasing Neon density at the NP and almost unchanged Neon core content. As far as Carbon is concerned, the situation is more complicated, due to the complex generation mechanisms, which depend on the edge conditions. However, a first approach has been made with simulations of Nitrogen injection experiments, since Nitrogen is, like Carbon, a non recycling, chemically active species. The BBQ simulations for Nitrogen show the same type of flux distribution as in the Neon case, with a strong outflux from the ergodic region to the edge.

7. Conclusion

The effect of the edge electron temperature (and density) has been shown on Carbon and Neon screening in ergodic divertor experiments. The measurements show that for Carbon, the screening effect is related to the generation process and localised within the laminar layer, whereas for Ne there is no sign of screening close to the NP. A heuristic model allows to confirm this observation by indicating an effective width of the edge screening region of less than 2 cm for Carbon and close to 20 cm for Ne. In order to interpret these results in terms of transport, BBQ 3D modelling of the ill-confined plasma edge coupled to the 1D code MIST for the confined plasma has been performed. It suggests that strong outfluxes from the ergodic region to the edge tend to shield the core from Ne. To confirm this preliminary interpretation, a comparison of the code results with the spectroscopic measurements of the intermediate ionisation stages is necessary.

References

[1] P. Monier-Garbet et al., J. Nucl. Mater. 266-269 (1999) 611.
[2] C. Grisolia et al., 14th International Conference on Pasma-Surface Interactions in Controlled Fusion Devices, Rosenheim (2000), to be published in J. Nucl. Mater.
[3] J.C. Valllet, 14th International Conference on Pasma-Surface Interactions in Controlled Fusion Devices, Rosenheim (2000), to be published in J. Nucl. Mater.
[4] W. Eckstein, J. Nucl. Mater. 248 (1998) 1.
[5] P. Ghendrih et al., Plasma Phys. Control. Fusion 38 (1996) 1653.
[6] J. Gunn et al., Plasma Phys. Control. Fusion 41 (1999) B243.
[7] J. Hogan et al., Proceedings of the 16th IAEA International Conference on Plasma Physics and Controlled Fusion Research, Vol. 2, Montreal 1996, p. 625.
[8] R. Hulse, Nuclear Technology / Fusion 3 (1983) 259.
[9] M. Bécoulet et al., Contrib. Plasma Phys. 40 (2000) 3-4, 251.
[10] W. Hess et al., Proceedings of the 27th International EPS Conference on Controlled Fusion and Plasma Physics, Budapest 2000.
[11] H.P. Summers, JET internal report JET-IR (94)06

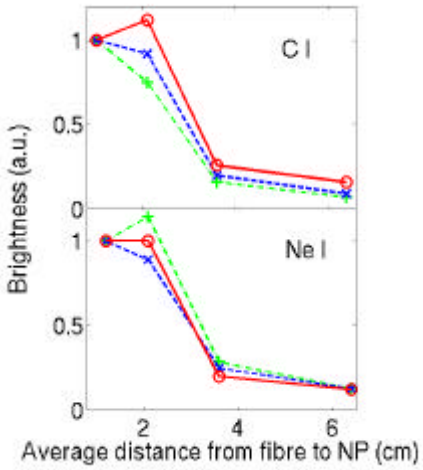

Fig. 1: C I (9080 Å multiplet) and Ne I (5852 Å) brightness profiles; solid line: T_e^{edge} = 60 eV, dashed line: T_e^{edge} = 40 eV, dotted line: T_e^{edge} = 20 eV.

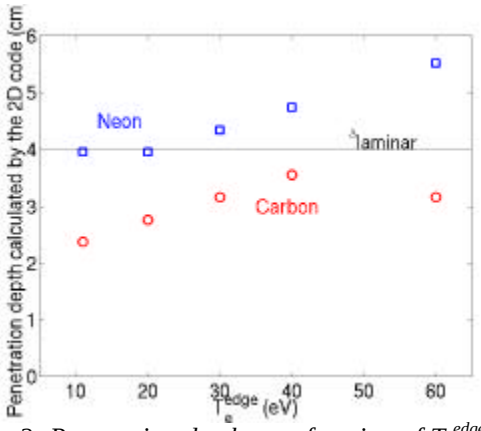

Fig. 2: Penetration depth as a function of T_e^{edge}, as calculated by the 2D code.

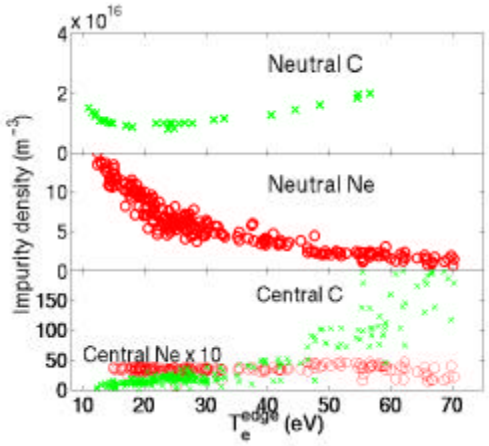

Fig. 3: Neutral C (top) and Ne (middle) densities and corresponding central densities (bottom).

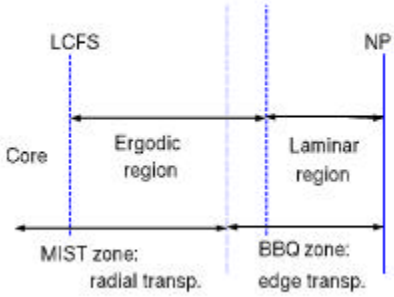

Fig. 4: Plasma edge transport in ED configuration and code utilisation.

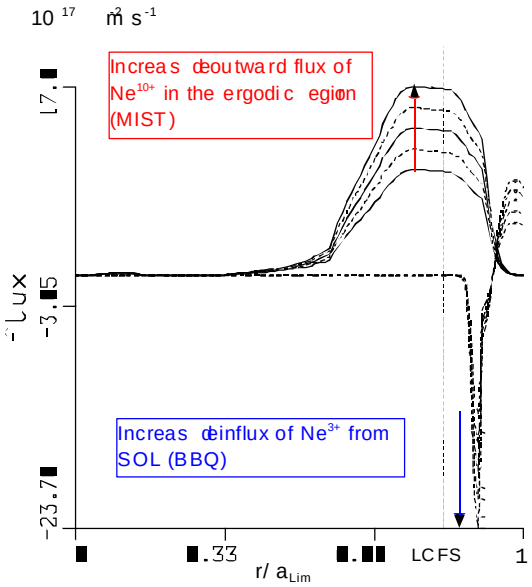

Fig. 5: Radial flux profiles for Ne^{3+} and N^{e10+} for increasing densities